Origin of the Relaxor State in $Pb(B_xB'_{1-x})O_3$ Perovskites

Silvia Tinte,[1] B. P. Burton,[1] Eric Cockayne,[1] and U. V. Waghmare[2]

[1]*Ceramics Division, Materials Science and Engineering Laboratory, National Institute of Standards and Technology, Gaithersburg, Maryland 20899-8520, USA*

[2]*J. Nehru Theoretical Sciences Unit, JNCASR, Jakkur, Bangalore, 560 064, India*

(Received 10 May 2006; published 29 September 2006)

Molecular dynamics simulations of first-principles-based effective Hamiltonians for $Pb(Sc_{1/2}Nb_{1/2})O_3$ under hydrostatic pressure and for $Pb(Mg_{1/3}Nb_{2/3})O_3$ at ambient pressure show clear evidence of a relaxor state in both systems. The Burns temperature is identified as the temperature below which dynamic nanoscale polar clusters form, pinned to regions of quenched chemical short-range order. The effect of pressure in $Pb(Sc_{1/2}Nb_{1/2})O_3$ demonstrates that the stability of the relaxor state depends on a delicate balance between the energetics that stabilize normal ferroelectricity and the average strength of random local fields which promote the relaxor state.

DOI: 10.1103/PhysRevLett.97.137601 PACS numbers: 77.80.Bh, 61.46.−w, 64.70.Kb, 77.84.Dy

Perovskite-based $A(B_{1/2}B'_{1/2})O_3$ and $A(B_{1/3}B'_{2/3})O_3$ relaxor ferroelectrics (RFE) [1,2], such as $Pb(Sc_{1/2}Nb_{1/2})O_3$ (PSN) and $Pb(Mg_{1/3}Nb_{2/3})O_3$ (PMN), are technologically important transducer or actuator materials with extraordinary dielectric and electromechanical properties. Unlike a normal ferroelectric (FE) [3], the dielectric constant of a RFE exhibits a high peak, over a broad temperature range, with strong frequency dispersion, which clearly indicates relaxation processes at multiple time scales [4]. It is generally accepted that RFE properties are associated with an intrinsic local structure of polar nanoregions (PNR) [5,6], the precise nature of which remains controversial. Phenomenological models for solids with random chemical disorder show how local dipole moments (e.g., off-centered ions) in a polarizable lattice can lead to relaxor behavior [7], but do not address nanoscale short-range chemical order that enhances relaxor properties in the important family of $Pb(B_xB'_{1-x})O_3$ perovskites [8]. Previous simulations [9,10] of microscopic models for PSN and PMN indicated a very strong spatial correlation between PNR and short-range chemically ordered regions, but no conclusive evidence of a relaxor state was found; e.g., the Burns temperature T_B [11] was not located. In this Letter, we present first-principles-based simulations of PSN under pressure and of PMN at ambient pressure that clearly exhibit a relaxor state in the paraelectric phase. An analysis of the short- to medium-range polar order allows us to locate T_B. Below T_B, the relaxor state is characterized by enhanced short- to medium-range polar order (PNR) pinned to nanoscale chemically ordered regions. The calculated temperature-pressure phase diagram of PSN demonstrates that the stability of the relaxor state depends on a delicate balance between the energetics that stabilize normal ferroelectricity and the average strength of quenched "random" local fields.

Simulations were performed using the first-principles-based effective Hamiltonian H_{eff} described in detail in [10], which expands the potential energy of PSN in a Taylor series about a high-symmetry perovksite reference structure, including those degrees of freedom relevant to ferroelectric phase transitions:

$$H_{\text{eff}} = H(\{\vec{\xi}_i\}) + H(e_{\alpha\beta}) + H(\{\vec{\xi}_i\}, e_{\alpha\beta}) + PV + H(\{\vec{\xi}_i\}, \{\sigma_l\}), \quad (1)$$

with $\{\vec{\xi}_i\}$ representing local polar distortion variables centered on Pb sites, $e_{\alpha\beta}$ the homogeneous strain, $H(\{\vec{\xi}_i\}, e_{\alpha\beta})$ a strain coupling term, and PV the standard pressure-volume term. These first four terms constitute a valid H_{eff} for modeling pressure-dependent phase transitions in a normal FE perovskite without local fields [12]. The fifth term, $H(\{\vec{\xi}_i\}, \{\sigma_l\})$, is a random local field term [13,14], proportional to $\sum_i \vec{h}_i \cdot \vec{\xi}_i$, where $\vec{h}_i$ is the local electric field at Pb site i created from the screened electric fields of the quenched distribution of Sc and Nb ions $\{\sigma_l\}$.

Molecular dynamics (MD) simulations were performed on a H_{eff} for PSN in a 40^3 unit cell simulation box for which $P = 0$ results were already presented [9]. The quenched chemical, and therefore $\vec{h}_i$ microstructure, of the simulation box consists of 20 chemically ordered regions (COR) in a percolating disordered matrix (PDM). The chemical microstructure was chosen to correspond to experimental observations of approximately 2 to 5 nm diameter chemically ordered nanodomains in Pb-based relaxors [8]. To obtain PDM statistics directly comparable to COR statistics, the PDM was subdivided into 60 "chemically disordered regions" (CDR). Each COR, and CDR, contains 800 Pb sites in an approximately spherical volume. Figure 1 is a (110) cross section through the simulation box, in which arrows represent projected $\vec{h}_i$. The COR are the roughly circular regions in Fig. 1 that have relatively low and homogeneous $\vec{h}_i$. The CDR that make up the PDM have larger more varied and intense $\vec{h}_i$.

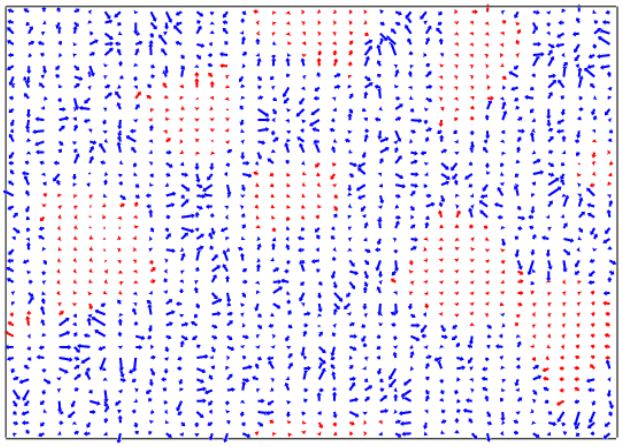

FIG. 1 (color online). A (110) plane through the PSN simulation box representing the projected local field (arbitrary units) at each Pb site in the plane. Chemically ordered regions (approximately circular) have small approximately homogeneous fields, and chemically disordered regions have larger more varied and disordered local fields.

MD simulations were also performed, at ambient pressure, for a PMN model [10]; here, we reanalyze these results. These simulations use the same effective Hamiltonian with the same arrangement of COR and CDR as in the PSN model, except that the COR for PMN have 1:1 ''random site'' ordering [15], i.e., a Nb sublattice alternating with a random $Mg_{2/3}Nb_{1/3}$ sublattice.

Figure 2 plots PSN bulk polarization as a function of T at various pressures in the range $0 < P < 22$ GPa. At each pressure below 22 GPa, a first-order transition is observed at the temperature at which the polarization jumps. The first-order character of the transition becomes stronger as P increases and the transition temperature approaches zero. A region with polarization departing from zero appears above the low-temperature phase and enlarges in T range as pressure increases.

Figure 3(a) plots histograms of a representative polarization component in the COR of the 18 GPa simulation at three temperatures. Above the temperature at which polarization differs noticeably from zero (320 K), the distribution is unimodal, centered at zero. In the ''pretransition'' region, (120 K), the distribution is bimodal with two unequal peaks at nonzero values. Below the first-order phase transition (80 K), the distribution is unimodal again but centered at a nonzero value. We interpret these results as indicating that, at 18 GPa, the system is paraelectric (PE) at 320 K, in a relaxor state at 120 K, and ferroelectric (FE) at 80 K. The asymmetric distribution of polarization in the relaxor state and resultant bulk polarization is likely a finite size effect (the simulation box only contains 20 chemically ordered regions); in the limit of infinite simulation box, the relaxor state should have zero bulk polarization. We associate the experimental Burns temperature T_B [11] with the temperature below which the COR become polar. Because the histogram method is cumulative over both space and time, it identifies static *or* dynamic polar clusters. At least for temperatures approaching T_B, some reorientations of the polarizations of individual polar clusters occurs during 48 ps simulation time, indicating the existence of dynamic polar clusters.

Similar effects are seen in Fig. 4, a plot of T-dependent dot products of cluster polarizations, $\langle \vec{S}_i(t) \cdot \vec{S}_j(t) \rangle$, at different pressures. $\vec{S}_i(t)$ is the MD spatial averaged polarization on an 800 site cluster that is either a COR ($i \rightarrow O$) or a CDR ($i \rightarrow D$), and $\langle\rangle$ indicates time averaging over a 48 ps MD simulation. These products clearly show the increase in pretransition polar short-range order which identifies the

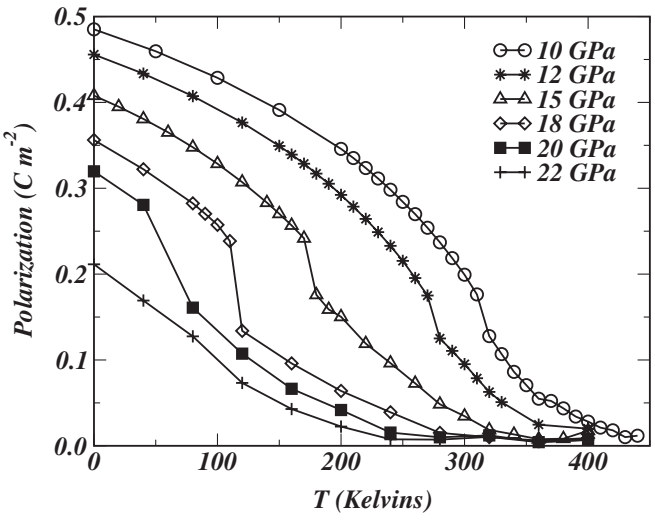

FIG. 2. Simulated PSN polarization as a function of temperature at hydrostatic pressures in the range $0 < P < 22$ GPa.

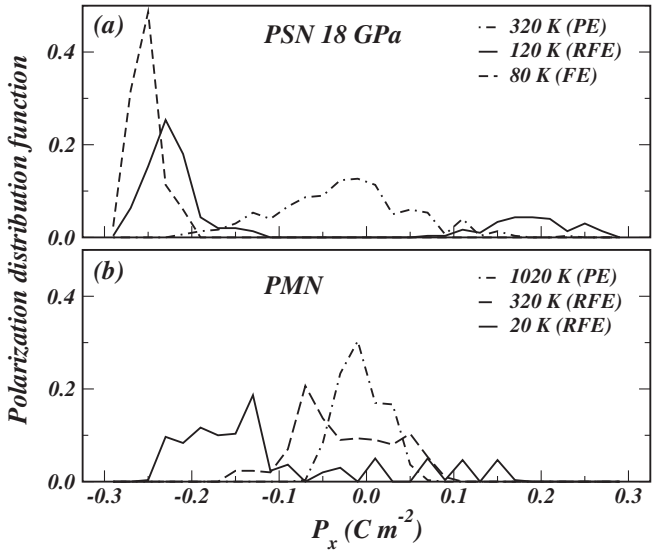

FIG. 3. Cumulative histogram of P_x values for chemically ordered regions at different temperature in the (a) 18 GPa PSN and (b) PMN simulations. The three curves in (a) correspond to paraelectric, relaxor, and ferroelectric states.

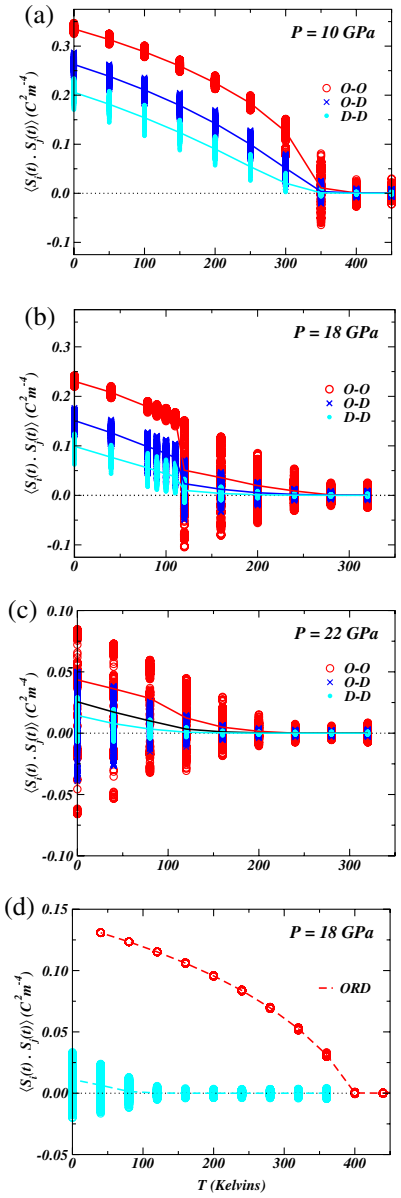

FIG. 4 (color online). PSN cluster-polarization dot products as functions of temperature: *O-O* indicate products between moments of two chemically ordered clusters, $\langle \vec{S}_O(t) \cdot \vec{S}_{O'}(t) \rangle$; *O-D* for products between one chemically ordered and one disordered cluster, $\langle \vec{S}_O(t) \cdot \vec{S}_D(t) \rangle$; *D-D* is for two disordered clusters, $\langle \vec{S}_D(t) \cdot \vec{S}_{D'}(t) \rangle$. Lines link average products. (a) At 10 GPa the relaxor region is small. (b) At 18 GPa there is a substantial relaxor region above a first-order phase transition. (c) At 22 GPa the transition is suppressed, and only the relaxor region persists. (d) is a plot of the $P = 18$ GPa results for: an ideally ordered system (above) which has no quenched local fields and a chemically random configuration (below).

RFE state, with both positive and negative dot products between ordered regions in the RFE state because of the absence of long-range polar order. Below the FE transition temperature, the cluster-cluster dot products are all positive owing to long-range polar order. The polarization dot products between CDR are small and centered near zero except below the FE transition temperature. Our results show that the COR control the behavior of the relaxor state and that strong $\vec{h}_i$ hinder cooperative Pb displacements and polarization fluctuations in the disordered matrix.

For comparison, Fig. 4(d) is a plot of the $P = 18$ GPa results for PSN with ideal 1:1 and with random chemical order. For ideal chemical order, all $\vec{h}_i = 0$, hence the collapse of isothermal variation in cluster-polarization dot products, and a sharp PE-FE phase transition. The chemically random configuration has a greater average value for local fields, $\langle |\vec{h}_i| \rangle$, than configurations with COR, and therefore exhibits cluster-polarization dot products similar to those of the nanoscale-ordered system at $P = 22$ GPa. It has been observed experimentally that chemical inhomogeneity enhances relaxor properties [8]. While the 18 GPa results in Fig. 4 support this conclusion, polarization in nm-sized regions of random PSN at low temperatures, plus results for random PSN at zero pressure [16], suggest some relaxor character even in a chemically random system.

The results in Fig. 2–4 were used to construct the P versus T phase diagram (Fig. 5): the FE $\rightleftharpoons$ RFE phase boundary (locus of T_{FE}) was estimated from Fig. 2; the RFE $\rightleftharpoons$ PE *crossover* (locus of T_B) [17] was estimated from the temperatures at which distributions of COR polarization components changed from unimodal above to bimodal below.

Experimentally, PSN that is cooled at ambient pressure exhibits RFE properties between ~365 K and ~400 K, below which it transforms to a FE phase [18]. Increasing pressure increases the temperature range of the RFE state and lowers the transition temperatures [19,20]. Qualitatively, the results presented above are fully consistent with experiment, although we see no evidence for termination of the FE $\rightarrow$ RFE transition line at an isolated critical point as *suggested* by [19]. Quantitatively, several

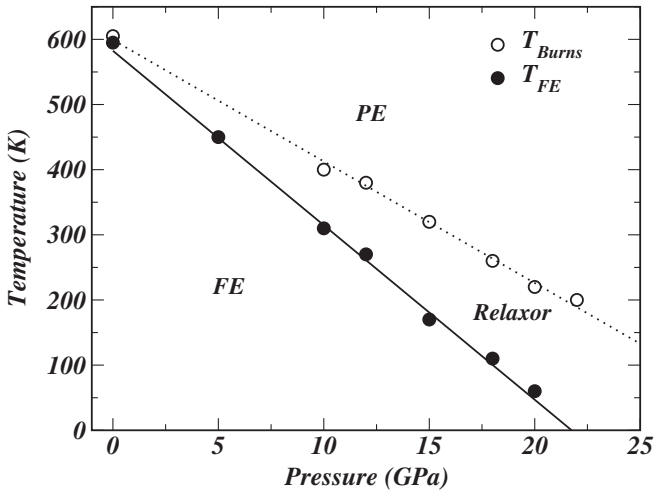

FIG. 5. Predicted pressure vs temperature phase diagram for PSN, indicating the ferroelectric to relaxor transition and the estimated Burns temperature.

sources of error affect predicted transition temperatures, while having no qualitative effect on our conclusions: (1) errors in first-principles calculations; (2) omission of anharmonic couplings with ionic degrees of freedom not included in H_{eff}, e.g., Nb displacements [21]; (3) treatment of local electric fields as P independent, when in fact they vary as the inverse square of the lattice constant, though the increase in $\langle h_i \rangle$ at 20 GPa is less than 5%. In addition, a more realistic representation of the chemical short-range order (a distribution of sizes and shapes of COR; less than perfect order within the COR) should result in a more gradual RFE $\rightleftharpoons$ PE crossover.

The simulations that were used to calculate Fig. 5 also omitted zero-point corrections [22] which were shown to lower transition temperatures, and to cause near infinite slopes in the phase boundaries of the pressure-temperature phase diagram for $BaTiO_3$ ($dT_{\mathrm{FE}}/dP \rightarrow \infty$ as $T_{\mathrm{FE}} \rightarrow 0$), as observed experimentally [23]. Because zero-point corrections only affect the normal FE part of H_{eff}, they should have the same effect on the FE $\rightarrow$ RFE phase boundary and the RFE $\rightarrow$ PE crossover in our model.

Polarization histograms for the ambient pressure PMN study [10] are shown in Fig. 3(b). The results show evidence for a PE-RFE crossover, but no FE phase appears even at low temperatures. Variability in the PMN polarization distribution is larger than that for PSN. This reflects significantly stronger random local fields in PMN, both from the larger charge difference, Mg^{2+} and Nb^{5+} in PMN versus Sc^{3+} and Nb^{5+} in PSN; and from significant $Mg_{2/3}Nb_{1/3}$-sublattice disorder in COR in the random site model [10,15]. For PMN, our calculated $T_B = 400$ K is less than the experimental value of 670 K [11]. Despite errors in characteristic temperatures, the experimental phase diagrams of both PSN and PMN, including the relaxor state, are qualitatively reproduced.

As discussed by Burton *et al.* [10] the competition between normal FE and RFE states is governed by the relative strengths of the interactions that stabilize normal ferroelectricity, and the spatial average strength of quenched local fields, $\langle |\vec{h}_i| \rangle$, that promote the RFE state. Pressure smoothly and monotonically reduces FE well depths [24–26] thus reducing the stability of the normal FE phase, but it leaves the local fields essentially unchanged. Thus, an increase in pressure corresponds to a *relative increase* in $\langle |\vec{h}_i| \rangle$, by reducing the competing FE-stabilizing interactions. Therefore, increasing pressure drives a FE system that has sufficient local fields towards a fully RFE state without a FE ground state. In PMN, local fields are larger than in PSN, and both our model and experiment exhibit a fully relaxor state even at ambient pressure.

[1] G. A. Smolenskii and A. I. Agranovskaya, Fiz. Tverd. Tela **1**, 1562 (1959) [Sov. Phys. Solid State **1**, 1429 (1959)].
[2] L. E. Cross, Ferroelectrics **76**, 241 (1987).
[3] M. E. Lines and A. M. Glass, *Principles and Applications of Ferroelectrics and Related Materials* (Clarendon, Oxford, 1979).
[4] G. A. Samara, Phys. Rev. Lett. **77**, 314 (1996); J. Appl. Phys. **84**, 2538 (1998); *Fundamental Physics of Ferroelectrics 2000*, edited by R. E. Cohen (American Institute of Physics, New York, 2000), p. 344; J. Phys. Condens. Matter **15**, R367 (2003).
[5] R. Blinc, V. V. Laguta, and B. Zalar, Phys. Rev. Lett. **91**, 247601 (2003).
[6] I. K. Jeong *et al.*, Phys. Rev. Lett. **94**, 147602 (2005); B. Dkhil *et al.*, Phys. Rev. B **65**, 024104 (2001); P. M. Gehring, S. Wakimoto, Z. G. Ye, and G. Shirane, Phys. Rev. Lett. **87**, 277601 (2001).
[7] B. E. Vugmeister and H. Rabitz, Phys. Rev. B **57**, 7581 (1998); B. E. Vugmeister, Phys. Rev. B **73**, 174117 (2006).
[8] C. A. Randall and A. S. Bhalla, Jpn. J. Appl. Phys. **29**, 327 (1990).
[9] B. P. Burton, E. Cockayne, and U. V. Waghmare, Phys. Rev. B **72**, 064113 (2005).
[10] B. P. Burton, E. Cockayne, S. Tinte, and U. V. Waghmare, Phase Transit. **79**, 91 (2006).
[11] G. Burns and F. H. Dacol, Solid State Commun. **48**, 853 (1983).
[12] W. Zhong, D. Vanderbilt, and K. M. Rabe, Phys. Rev. Lett. **73**, 1861 (1994); K. M. Rabe and U. V. Waghmare, Phys. Rev. B **52**, 13 236 (1995); U. V. Waghmare and K. M. Rabe, Phys. Rev. B **55**, 6161 (1997).
[13] U. V. Waghmare, E. Cockayne, and B. P. Burton, Ferroelectrics **291**, 187 (2003).
[14] B. P. Burton, U. V. Waghmare, and E. Cockayne, TMS Letters **1**, 29 (2004).
[15] P. K. Davies and M. A. Akbas, J. Phys. Chem. Solids **61**, 159 (2000).
[16] R. Hemphill, L. Bellaiche, A. Garcia, and D. Vanderbilt, Appl. Phys. Lett. **77**, 3642 (2000); J. Íñiguez and L. Bellaiche, Phys. Rev. B **73**, 144109 (2006).
[17] The term *crossover* implies that RFE properties become measurable below T_B, and asymptotically approach zero above T_B. It also implies that the RFE state is a definable subspace of the paraelectric phase, but it is not a phase in the Gibbsian sense.
[18] F. Chu, I. M. Reaney, and N. Setter, J. Appl. Phys. **77**, 1671 (1995).
[19] E. L. Venturini, R. K. Grubbs, G. A. Samara, Y. Bing, and Z.-G. Ye, Phys. Rev. B (to be published).
[20] G. A. Samara and E. L. Venturini, Phase Transit. **79**, 21 (2006).
[21] O. Svitelskiy, J. Toulouse, G. Yong, and Z.-G. Ye, Phys. Rev. B **68**, 104107 (2003).
[22] J. Íñiguez and D. Vanderbilt, Phys. Rev. Lett. **89**, 115503 (2002).
[23] T. Ishidate, S. Abe, H. Takahashi, and N. Môri, Phys. Rev. Lett. **78**, 2397 (1997).
[24] R. E. Cohen, Nature (London) **358**, 136 (1992); R. E. Cohen and H. Krakauer, Ferroelectrics **136**, 65 (1992).
[25] G. Sághi-Szabó, R. E. Cohen, and H. Krakauer, Phys. Rev. Lett. **80**, 4321 (1998).
[26] M. Fornari and D. Singh, Phys. Rev. B **63**, 092101 (2001).